Journal of Physics:
Conference Series

Optical characterization of macro-, micro- and nanostructures using polarized light

Journal of Physics: Conference Series **558** (2014) 012008 doi:10.1088/1742-6596/558/1/012008

Optical characterization of macro-, micro- and nanostructures using polarized light

P Petrik[1,2], N Kumar[4], G Juhasz[1], C Major[1], B Fodor[1,3], E Agocs[1], T Lohner[1], S F Pereira[4], H P Urbach[4] and M Fried[1,2]

[1] Institute for Technical Physics and Materials Science, Research Centre for Natural Sciences, Konkoly Thege Rd. 29-33, 1121 Budapest, Hungary
[2] Doctoral School of Molecular- and Nanotechnologies, Faculty of Information Technology, University of Pannonia, Egyetem u. 10, Veszprém, H-8200, Hungary
[3] Faculty of Science, University of Pécs, 7624 Pécs, Ifjúság útja 6, Hungary
[4] Department of Imaging Physics, Faculty of Applied Sciences, Delft University of Technology, P. O. Box 5046, 2600GA Delft, The Netherlands

E-mail: petrik@mfa.kfki.hu

Abstract. Reflection of light measured in a polarimetric, scatterometric and spectroscopic way allows the measurement of structures in a broad size range from large (meter) scales like photovoltaic panels down to small (nanometer) scales like nanocrystals. Optical metrology continues to be improved to measure those materials with increasing sensitivity and accuracy, typically in a form of thin films on high quality substrates. This review provides an overview of some recently developed or improved methods, e.g. divergent light source ellipsometry for the mapping of large surfaces for photovoltaic applications, Fourier scatterometry for the measurement of periodic structures with sizes comparable to the wavelength of illumination, as well as spectroscopy around the band gap photon energies to characterize nanostructures – without attempting completeness.

1. Introduction

There is a huge variety of optical metrologies for a large number of applications. One peculiarity of optical techniques is that the measurable feature sizes cover a range from sub-wavelength dimensions to large scales. While there is no upper size limit for imaging (e.g. astronomical telescopes), imaging of thin film properties with high accuracy on large surfaces is currently a hot topic, due to display and solar panel applications. For layer thicknesses larger than the wavelength of illumination, reflectometry is a simple and robust method. However, by measuring the phase between the reflections polarized parallel and perpendicular to the plane of incidence, the sensitivity can largely be increased and sub-wavelength layer thicknesses (even below one nanometer) can be measured [1–5].

These polarimetric techniques can be realized in a broad variety of instrumental configurations, of which one of the most popular and simple is rotating polarizer/analyzer ellipsometry [3]. Ellipsometric imaging has been realized in many configurations including microscopic imaging combined with spectroscopic ellipsometry for e.g. biosensors or graphene mapping [6–9], using translation stages or moving the complete ellipsometry heads over the

sample to map it spot-by-spot [10, 11], or imaging large areas using extended illumination, as demonstrated in the case of divergent light source ellipsometry [12–18] in the next chapter.

If the characteristic feature size of the structures to be measured is close to the wavelength of illumination, scattering and diffraction can be utilized. Under these circumstances, the interaction between light and matter results in a characteristic pattern of the electric far field measured as a function of the reflection angle. This pattern can also be calculated using optical models of the structure and the structural parameters, which are much smaller than the resolution limit of geometrical optics, can be determined with high accuracy. The limitation is that this method can only be used for periodic structures. Optical diffraction and scattering measurements have been utilized extensively for a long time, using versatile configurations from goniometric scatterometry to Fourier scatterometry [19–27]. In Chapter 3, the latter method will be discussed briefly.

Finally, when the size of structures (e.g. semiconductor nanocrystals) is much smaller than the wavelength of the light used for the measurement, the characteristic size can be determined indirectly, by the influence of the crystal size on the electron band structure. When using spectroscopy and measuring dielectric functions in photon energy ranges close to the interband transition energies, the band structure can be scanned, since the imaginary part of the dielectric function is proportional to the joint density of electron states. Around the critical points of direct interband transition energies, the change of nanostructure has a large influence on the dielectric function, which allows a sensitive way of crystal size measurement (as discussed in Chapter 4) [4, 5, 28–38].

2. Mapping of large surfaces ($d > \lambda$)

From the viewpoint of optical characterization, a straightforward choice is to distinguish the regions of "macro", "micro" and "nano" features by the relation between the feature size (d) and the wavelength of illumination (λ), as shown in the headings of this and the following chapters. In this chapter, we most specifically focus on the cases of $d \gg \lambda$ with the aim of extending the size, speed and precision of large area thin film measurement (most importantly for photovoltaic applications [11, 15, 17], but large displays and 450 mm wafer activities are significant targets as well).

Wafer mapping has been required in microelectronics for a long time (see e.g. Ref. [39] for ion implantation). The most sensitive optical mapping techniques involve polarimetry in a broad range of wavelengths and configurations [10–12, 15, 17, 40–58] (note that the sensitivity of polarimetric techniques allows not only a lateral but also a vertical depth profiling [59–62]). The most common and major approach, which emerged first and continues to be used, is to scan either the sample stage or the optical heads over the sample to measure point-by-point [10, 11, 47, 48, 50–53, 63] (even with microfocus-infrared [45]). A newer and nowadays rapidly improving method is imaging, which has been developed to measure areas from small [7, 9, 43, 54, 55, 57] to ever increasing sizes [12, 15, 17, 18, 49, 58]. It has to be pointed out that, parallel to instrumental development, optical modeling techniques are also undergoing a significant improvement [1–5, 64].

Film thickness imaging on large scales is challanging for several reasons. First of all, the flatness of the sample has to be minimized and/or taken into account. Second, the beam path and the optical configuration usually has to be adapted to a specific application. In some cases the sample to be investigated can be placed onto a large mapping tool [11], but for *in line* or even *real time* applications special constraints have to be taken into account, as demonstrated in figures 1 and 2. Both are utilizations of the spectroscopic line-scan version of divergent light source mapping ellipsometry [12, 15, 18] for *in line* applications. In these configurations a line-scan is realized, whereas the second index of the detector is used for spectroscopic information. In the arrangement of figure 1, 30 points of a 450 mm diameter wafer have to be measured

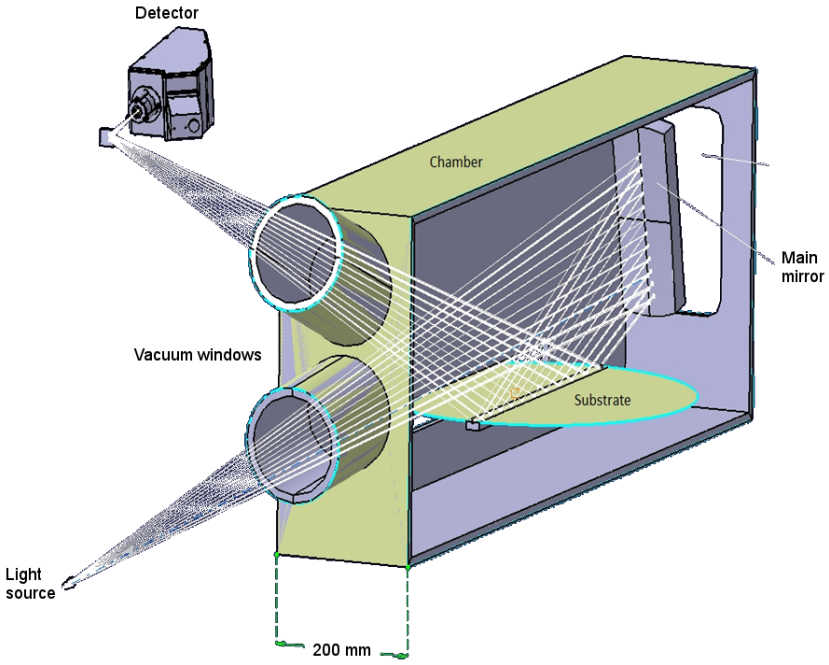

Figure 1. Integration of divergent light source mapping ellipsometry into a transport module of a cluster chamber. The substrate to be measured in the chamber has a diameter of 450 mm.

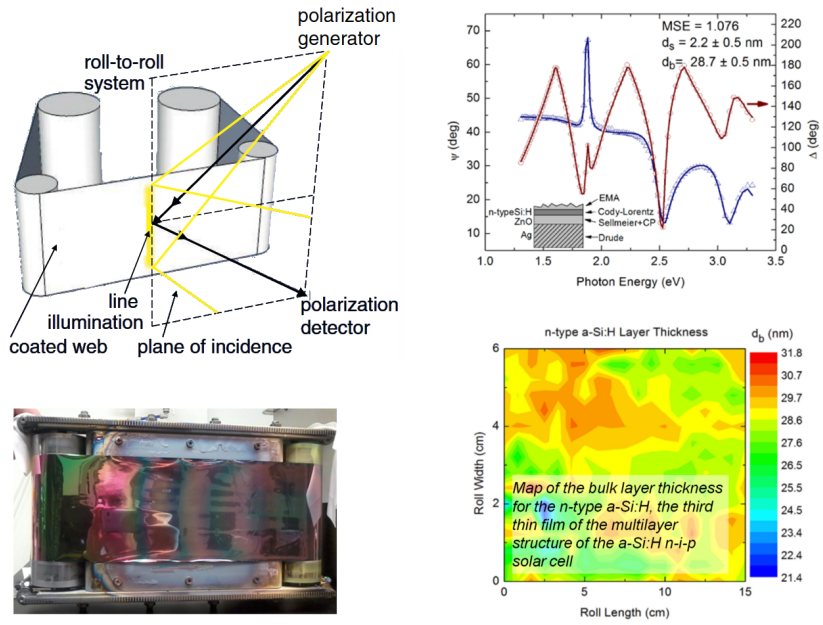

Figure 2. 2D-mapping by divergent light source ellipsometry in a roll-to-roll arrangement (top left). The equipment with the foil on the rolls is shown in the bottom left image. The measured and fitted spectra at one point of a line scan is shown in the top right graph, together with the optical model (see the inset). The determined thickness map is shown in the bottom right graph.

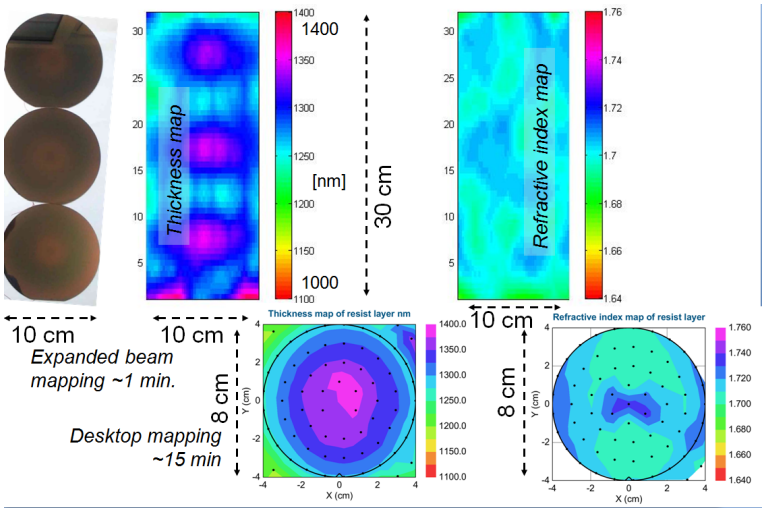

Figure 3. Thickness and refractive index maps using a line scan during translation (bottom graphs), verified by desktop mapping (bottom graphs).

along a line simultaneously, in the wavelength range of 350-1000 nm, within several seconds.[1] The 2D mapping can be realized by measuring along the line while moving the wafer in the transport module. This mapping is basically identical to that used for roll-to-roll mapping, as demonstrated in figure 2. One line is measured simultaneously in a broad wavelength range, and the mapping is performed by translating the roll, which can be part of the production procedure – this makes the tool integrable into an industrial environment in a straightforward way.

Currently, a line scan of 30 points during a translation of 10 cm can be measured within 1 minute, as shown in figure 3. The spectroscopic capability also allows the determination of the refractive index as a map. One of the near-future goals of the project is to scan a 60-cm line, and increase the speed so that, with a suitable traversal time, a 60 cm $\times$ 120 cm photovoltaic panel can be measured in 1800 points within $\approx$1 minute [18].

3. Metrology of photonic structures ($d \sim \lambda$)

Scatterometry has been applied for the measurement of microsctructure and periodic feature sizes for decades [27, 65–67]. As for large area thin film mapping presented in the previous chapter, polarimetry has an added value in this case as well, most importantly in terms of precision (e.g. critical dimension ellipsometry [68, 69] or infrared scattering ellipsometry [70]). The used angle and wavelength ranges as well as configurations cover a wide range, depending on the applications.

In this chapter we focus on Fourier scatterometry [19–27], which has the unique capability of measuring a broad range of scattering angles simultaneously, by illuminating and measuring using the same high numerical aperture objective (for the optical setup see figure 4). Using coherent illumination, the light is focused on the periodic structure with a spot size which is comparable with the period of the structure. When the sample is in focus, the intensity in each point of the back focal plane of the microscope objective uniquely corresponds to a given angle of reflection [19]. Therefore, by imaging the back focal plane of the objective, the spatial distribution of the intensity pattern on the CCD is directly linked to the angle distribution of the light reflected from the sample [26]. It has been shown previously that coherent illumination

[1] As part of the ENIAC E450EDL project.

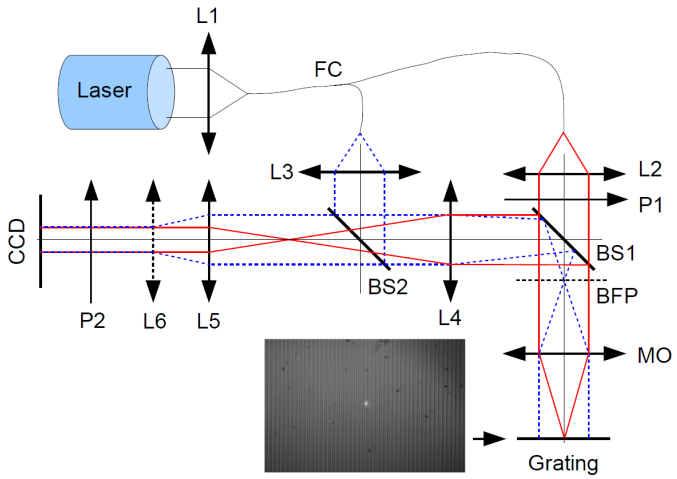

Figure 4. Setup of Fourier scatterometry. L1, L2, L3: collimating lences; L4, L5, L6: telescopic lenses; P1, P2: polarizers; BS1, BS2: beam splitters; MO: microscope objective; BFP: back focal plane; CCD: detector. The inset shows the case of imaging the grating to the CCD, together with the focused spot.

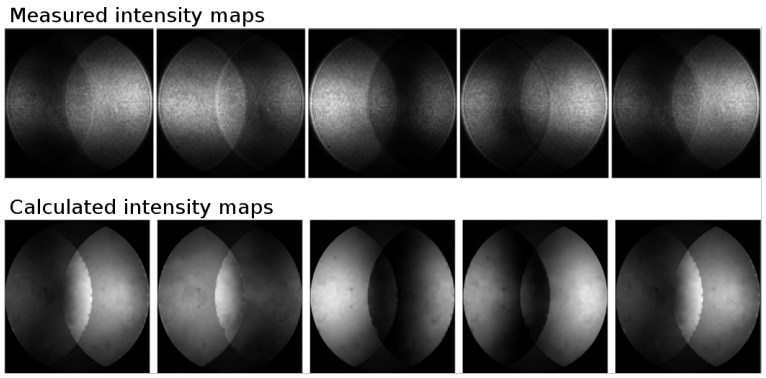

Figure 5. Measured (top row) and calculated (bottom row) far field intensity images for a 2-μm pitch silicon grating (duty cicle of 0.5) with a height of 148 nm, by scanning the focused spot evenly distributed over one period of the grating (represented by the different columns – the first and last images correspond to the same position with regard to the grating period). The wavelength of illumination was 633 nm.

provides a possibility of measuring the phase between the diffracted orders in the pupil, when properly scanning the focused spot along the investigated periodic structure. The capability of measuring the phase (as in the case of ellipsometry) increases the sensitivity significantly. The tool has recently been experimentally realized and the high sensitivity revealed [26].

Figure 5 shows a series of far field intensity images taken using different spot positions perpendicular to the grooves of a silicon grating. As emphasized for thin film mapping in the previous chapter, forward calculation of the far field based on a proper optical model is a crucial part of the procedure [71, 72]. Being a non-linear problem, *a priori* information on the structure is needed to have a suitable starting point of the evaluation procedure, from which the least squares method applied to the fit can converge to the global minimum. Comparison with

reference methods like scanning electron microscopy (SEM) and atomic force microscopy verify the reliability and accuracy being within several nanometers for sub-micron grating periodicities. Furthermore, based on the large sensitivity of the far field interference pattern on the position of the focused spot, the method can also be used for spot positioning with nanometer precision [26].

4. Characterization of nanostructures ($d < \lambda$)

The optical characterization of nanostructures is based on the fact that the structural change of the materials changes its dispersion, which can be measured using spectroscopy. More specifically, the imaginary part of the dielectric function is proportional to the joint density of electron states. Since the dielectric function can be measured with a typical accuracy of down to 10^{-4} using sensitive optical techniques, minute structural changes can be followed even *in situ*, if proper optical models can be built concerning the structure [73–76].

As emphasized above, according to the indirect nature of most optical characterization methods, the accuracy of structural characterization largely depends on the application of proper optical models. These models are usually verified by direct reference methods (e.g. SEM), however, as soon as the model is verified, optical methods are capable of the high-sensitivity, fast and non-destructive measurement of the nanostructures, which is applied e.g. as a powerful *in line* or *real time* inspection method during thin film preparation and device manufacturing [77].

The most frequently applied method for the optical modeling of nanostructure is the effective medium approximation (EMA [28, 78]), which describes the material as a composite of distinct phases with sizes much smaller than the wavelength of characterization, but large enough to have a characteristic dielectric function. The two major problems with EMA are that the dielectric function of components are frequently different from those that can be found in databases (because of different preparations or due to size effects) and the way the screening effect and the anisotropy due to the non-uniformity of phase boundaries are taken into account. Nevertheless, there is a huge number of publications using this theory, usually with results that are in good agreement with reference methods.

A nice example of EMA is the characterization of porous materials, as demonstrated in figure 6. The ellipsometric measurement of electrochemically etched thin films in silicon can be modeled using EMA with components of single-crystalline silicon and void, which can be extended by a fine-grained polycrystalline silicon reference if the typical crystallite sizes of the remaining porous Si skeleton are very small [37, 79, 80]. By fitting the volume fraction of void, the optical density and in turn the porosity can be determined, as demonstrated for void gradients caused by ion implantation [81, 82]. The sensitivity also allows the determination of density gradients within the thin films.

By measuring absorbing materials with large dispersion spectroscopically, the fact that the penetration depth depends on the absorption can be utilized, as demonstrated in figure 7. Semiconductors have absorption peaks at the so called critical point photon energies corresponding to direct interband transitions. Figure 7 shows this fact at the example of polycrystalline silicon, which has a large absorption peak in the ultraviolet spectral range at wavelengths of around 300 nm. In this range, the imaginary part of the refractive index (extinction coefficient, k) almost reaches 5, and the corresponding optical penetration depth (OPD) is well below 10 nm (right-hand side axis and dashed line in figure 7). However, when the wavelengh is increased (from the peak value of ≈300 nm), k drops at wavelengths of around 400 nm and the penetration depth rapidly increases, reaching a value of 500 nm (the thickness of the polycrystalline silicon layer) at a wavelength of ≈550 nm.

When fitting the spectra measured by ellipsometry on the polycrystalline silicon layer (transmission electron microscopy image shown on the right-hand side of the graph), the

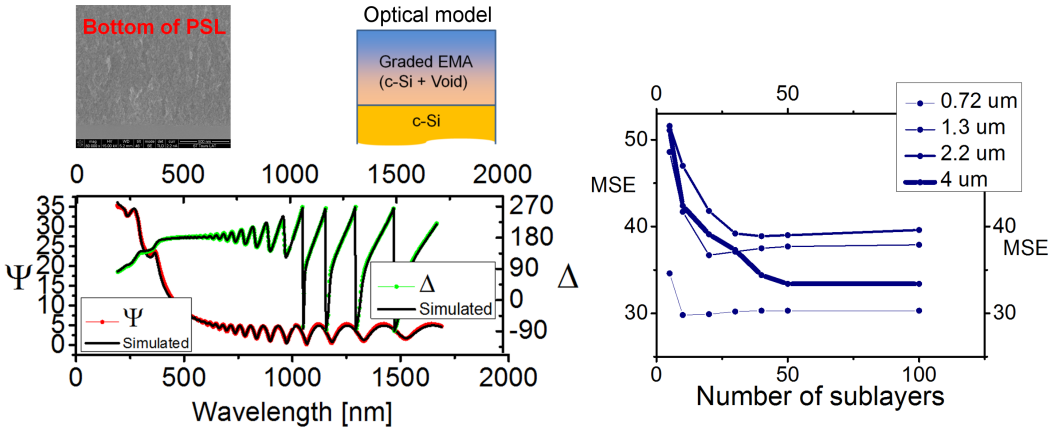

Figure 6. Graded effective medium model (insert at the top) for the characterization of porous silicon (top left image) with a thickness of ≈ 1.3 μm. The graph at the right-hand side shows that dividing the investigated layer into sub-layers, in order to determine void gradients, decreases the mean square error (MSE), i.e. increases the fit quality. However, using numerous sublayers may increase parameter correlations.

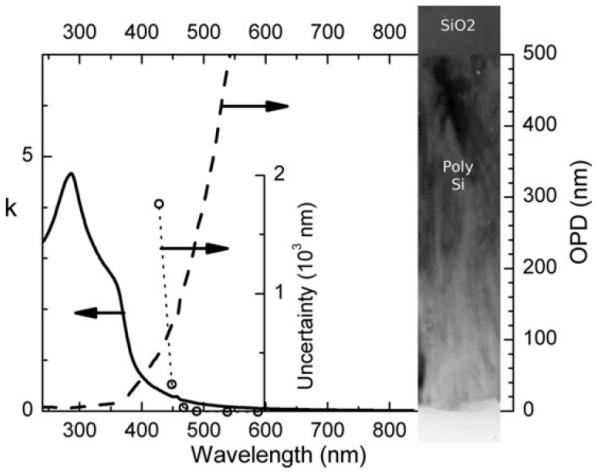

Figure 7. Extinction coefficient (k) and optical penetration depth (OPD) measured for an ≈500-nm polycrystalline silicon layer as a function of the wavelength, as well as the uncertainty of the fitted thickness of the polycrystalline silicon layer as a function of the upper limit wavelength of the range used for the fit [38].

uncertainty of the fitted layer thickness was determined for different wavelength ranges, in which the lowest wavelength was fixed at the value corresponding to the largest absorption (≈300 nm) and the highest wavelength was changed from 600 to 430 nm. The open circles connected with a dotted line show that the uncertainty increases when the upper limit of the wavelength range decreases with increasing absorption and with decreasing penetration depth, due to the fact that the light does not sense the bottom interface of the layer, because of the increased absorption. It is also clear that the "information depth" is significantly larger than the "penetration depth" (calculated by $\lambda/(4\pi k)$), because the uncertainty is still low at a wavelength of 450 nm for which

OPD predicts ≈100 nm, although the layer thickness is ≈500 nm. We have shown recently that this effect can be used for a depth scan when plotting the fitted layer parameters as a funtion of the penetration depth, whereas the penetration depth can be varied by properly changing the wavelength range used for the fitting [38].

5. Conclusions

It has been that optical characterization methods are capable of measuring structural properties on a wide scale of sizes from macroscopic features that are larger than the wavelength of the illumination, down to nanoscale sizes which are much smaller than the wavelength. These goals are reached using versatile techniques including spectroscopy, diffraction, geometrical optics and polarimetry. Note that some of these techniques can be combined. For example, making imaging ellipsometry specroscopically, nanostructural information can be detected for each measured lateral position [18]. Mapping of non-uniform samples can also be combined with Fourier scatterometry, and Fourier scatterometry can be combined with spectroscopy.

Acknowledgments

Support from ENIAC E450EDL and KMR_12_1_2012_0225 projects, as well as the Hungarian-French Intergovernmental S&T Cooperation Programme grant Nr. TÉT_10-1-2011-0754 and by CampusFrance in the frame of a Balaton PHC project are greatly acknowledged.

References

[1] Fried M, Lohner T and Petrik P 2001 *Handbook of surfaces and interfaces of materials* vol 4 ed Nalwa H S (San Diego: Academic Press)
[2] Tompkins H G and Irene E G (eds) 2005 *Handbook of ellipsometry* (Norwich, NY: William Andrew)
[3] Fujiwara H 2007 *Spectroscopic Ellipsometry: Principles and Applications* (New York: Wiley)
[4] Petrik P 2012 *Nanocrystals - Synthesis, Characterization and Applications* ed Neralla S (http://dx.doi.org/10.5772/48732: InTech)
[5] Petrik P and Fried M 2012 *Ellipsometry at the Nanoscale* ed Losurdo M and Hingerl K (Heidelberg: Springer-Verlag)
[6] Jin G, Jansson R and Arwin H 1996 *Rev. Sci. Instrum.* **67** 2930
[7] Vaupel M, Yunfeng S and Zhimin Y 2008 *phys. stat. sol.* **205** 772
[8] Qi C, Zhu W, Niu Y, Zhu H G Z G Y, Meng Y H, Chen S and Jin G 2009 *Journal of Viral Hepatitis* **16** 822
[9] Wurstbauer U, Röling C, Wurstbauer U, Wegscheider W, Vaupel M, Thiesen P H and Weiss D 2010 *Applied Physics Letters* **97** 231901
[10] Huang Z, Chen J, Sestak M N, Attygalle D, Dahal L R and Mapes M R 2010 *IEEE Proceedings – Conference Record of the IEEE Photovoltaic Specialists Conference* **82805** 1678
[11] Dahal L R, Huang Z, Salupo C, Podraza N J, Marsillac S and Collins R W 2011 *IEEE Proceedings – 37th IEEE Photovoltaic Specialists Conference* **89752** 182
[12] Juhasz G, Horvath Z, Major C, Petrik P, Polgar O and Fried M 2008 *phys. stat. sol. (c)* **5** 1081
[13] Major C, Juhasz G, Petrik P, Horvath Z, Polgar O and Fried M 2009 *Vacuum* **84** 119
[14] Fried M, Juhasz G, Major C, Petrik P, Polgár O, Horváth Z and Nutsch A 2011 *MRS Proceedings* **1323** 157
[15] Fried M, Juhasz G, Major C, Nemeth A, Petrik P, Polgar O, Salupo C, Dahal L R and Collins R W 2011 *Thin Solid Films* **519** 2730
[16] Nemeth A, Attygalle D, Dahal L R, Aryal P, Huang Z, Salupo C, Petrik P, Juhasz G, Major C, Polgar O, Fried M, Pecz B and Collins R W 2011 *MRS Proceedings* **1321** 267
[17] Shan A, Fried M, Juhasz G, Major C, Polgar O, Nemeth A, Petrik P, Dahal L R, Chen J, Huang Z, Podraza N J and Collins R W 2014 *IEEE Journal of Photovoltaics* **4** 355
[18] Fried M 2014 *Thin Solid Films* **in press**
[19] Boher P, Petit J, Leroux T, Foucher J, Desieres Y, Hazart J and Chaton P 2005 *SPIE Proceedings* **5752** 192
[20] El Gawhary O, Kumar N, Pereira S F, Coene W M J and Urbach H P 2011 *Applied Physics B* **105** 775
[21] Kumar N, El Gawhary O, Roy S, Kutchoukov V G, Pereira S F, Coene W and Urbach H P 2012 *SPIE Proceedings* **8324** 83240Q
[22] Roy S, El Gawhary O, Kumar N, Pereira S F and Urbach H P 2012 *Journal of the European Optical Society - Rapid Publications* **7** 12031
[23] Kumar N, El Gawhary O, Roy S, Pereira S F and Urbach H P 2013 *SPIE Proceedings* **8788** 87881P

[24] Kumar N, El Gawhary O, Roy S, Pereira S F and Urbach H P 2013 *Journal of the European Optical Society - Rapid Publications* **8** 13048
[25] Roy S, Kumar N, Pereira S F and Urbach H P 2013 *Journal of Optics* **15** 075707
[26] Kumar N, Petrik P, Ramanandan G K P, El Gawhary O, Roy S, Pereira S F, Coene W M J and Urbach H P 2014 *Optics Express* **accepted**
[27] Endres J, Kumar N, Petrik P, Henn M A, Heidenreich S, Pereira S F, Urbach H P and Bodermann B 2014 *SPIE Proceedings* **9132** 913208–1
[28] Aspnes D E 1982 *Thin Solid Films* **89** 249
[29] Aspnes D E, Studna A A and Kinsbron E 1984 *Phys. Rev. B* **29** 768
[30] Logothetidis S, Polatoglou H M and Ves S 1988 *Solid State Commun.* **68** 1075
[31] Boultadakis S, Logothetidis S and Ves S 1992 *J. Appl. Phys.* **72** 364
[32] Asinovsky L M 1993 *Thin Solid Films* **233** 210
[33] Flueraru C, Gartner M, Dascalu D and Rotaru C 1996 *J. Phys. III France* **6** 225
[34] Borghesi A, Giardini M E, Marazzi M, Sassela A and Santi G D 1997 *Appl. Phys. Lett.* **70** 892
[35] Petrik P, Fried M, Lohner T, Berger R, Biró L P, Schneider C, Gyulai J and Ryssel H 1998 *Thin Solid Films* **313-314** 259
[36] Petrik P, Lohner T, Fried M, Biró L P, Khánh N Q, Gyulai J, Lehnert W, Schneider C and Ryssel H 2000 *J. Appl. Phys.* **87** 1734
[37] Petrik P, Fried M, Vazsonyi E, Basa P, Lohner T, Kozma P and Makkai Z 2009 *J. Appl. Phys.* **105** 024908
[38] Petrik P, Agocs E, Volk J, Lukacs I, Fodor B, Kozma P, Lohner T, Oh S, Wakayama Y, Nagata T and Fried M 2014 *Thin Solid Films* **in press**
[39] Keenan W A, Johnson W H and Yarling C B 1991 *Nucl. Instr. and Methods* **B55** 230
[40] Ohtsuka Y and Oka K 1992 *SPIE Proceedings* **1746** 42
[41] Chang Y S and Li S S 1995 *Solid-State Electronics* **38** 197
[42] Boher P, Defranoux C, Bourtault S and Stehle J L 1999 *SPIE Proceedings* **3677** 845
[43] Zhan Q and Leger J R 2002 *Applied Optics* **41** 4443
[44] Oka K and Kaneko T 2003 *Optics Express* **11** 1510
[45] Gensch M, Korte E H, Esser N, Schade U and Hinrichs K 2006 *Infrared Physics & Technology* **49** 74
[46] Hinrichs K, Gensch M, Esser N, Schade U, Rappich J, Kröning S, Portwich M and Volkmer R 2007 *Anal. Bioanal. Chem.* **387** 1823
[47] Roodenko K, Mikhaylova Y, Ionov L, Gensch M, Stamm M, Minko S, Schade U, Eichhorn K J, Esser N and Hinrichs K 2008 *Appl. Phys. Lett.* **92** 103102
[48] Krüger H, Kemnitz E, Hertwig A and Beck U 2008 *phys. stat. sol. (a)* **205** 821
[49] Major C, Juhasz G, Horvath Z, Polgar O and Fried M 2008 *phys. stat. sol. (c)* **5** 1077
[50] Weber J W, Hinrichs K, Gensch M, van de Sanden M C M and Oates T W H 2011 *Appl. Phys. Lett.* **505** 358
[51] Sago Y and Fujiwara H 2012 *Japanese J. Appl. Phys.* **51** 10NB01–1
[52] Rosu D, Petrik P, Rattmann G, Schellenberger M, Beck U and Hertwig A 2013 *Thin Solid Films* **in press**
[53] Aryal P, Attygalle D, Pradhan P, Podraza N J, Marsillac S and Collins R W 2013 *IEEE Journal of Photovoltaics* **3** 359
[54] Nielsen M M B and Simonsen A C 2013 *Langmuir* **29** 1525
[55] Röling C, Thiesen P, Meshalkin A, Achimova E, Abashkin V, Prisacar A and Triduh G 2008 *Appl. Phys. Lett.* **92** 103102
[56] Hinrichs K, Furchner A, Rappich J and Oates T W H 2013 *J. Phys. Chem.* **387** 1823
[57] Necas D, Ohlidal I, Franta D, Cudek V, Ohlidal M, Vodak J, Sladkova L, Zajickova L, Elias M and Vizd F 2013 *Thin Solid Films* **in press**
[58] Koops R, Sonin P, van Veghel M and Gawhary O E 2014 *J. Opt.* **16** 065701
[59] Vanhellemont J, Roussel P and Maes H E 1991 *Nucl. Instr. Meth.* **55** 183
[60] Fried M, Lohner T, Aarnink W A M, Hanekamp L J and van Silfhout A 1992 *J. Appl. Phys.* **71** 2835
[61] Lynch S, Murtagh M, Crean G M, Kelly P V and O'Connor M 1993 *Thin Solid Films* **233** 199
[62] Petrik P, Polgar O, Fried M, Lohner T, Khanh N Q and Gyulai J 2003 *J. Appl. Phys.* **93** 1987
[63] Berge C, Krasilnikova A and Masetti E 2000 *SPIE Proceedings* **4099** 319
[64] Fried M, Lohner T and Gyulai J 1997 *Effect of Disorder and Defects in Ion-Implanted Semiconductors: Optical and Photothermal Characterization* Semiconductors and Semimetals ed Cristofides C and Ghibaudo G (New York: Academic Press)
[65] Wurm M, Pilarski F and Bodermann B 2010 *Review of Scientific Instruments* **81** 023701
[66] Gross H, Richter J, Rathfeld A and Bär M 2010 *Journal of the European Optical Society Rapid Publications* **5** 10053
[67] Endres J, Bodermann B, Dai G, Wurm M, Henn M, Gross H, Scholze F and Diener A 2013 *Fringe Proceedings*

DOI: 10.1007/978-3-642-36359-7-128 695
[68] Hingst T, Marschner T, Moert M, Homilius J, Guevremont M, Hopking J and Elazami A 2003 *SPIE Proceedings* **5038** 274
[69] Huang H T and Terry F L 2004 *Thin Solid Films* **455-456** 828
[70] Guittet P Y, Mantz U and Weidner P 2004 *IEEE Proceedings - International Symposium on Semiconductor Manufacturing* **63503** 176
[71] Gross H, Model R, Bär M, Wurm M, Bodermann B and Rathsfeld A 2006 *Measurement: Journal of the International Measurement Confederation* **39** 782
[72] Model R, Rathsfeld A, Gross H, Wurm M and Bodermann B 2008 *J. Phys.: Conf. Series* **135** 012071
[73] Collins R W and Yang B Y 1989 *J. Vac. Sci. Technol.* **B7** 1155
[74] Collins R W, An I, Nguyen H V and Lu Y 1993 *Thin Solid Films* **233** 244
[75] Koh J, Fujiwara H, Koval R J, Wronski C R and Collins R W 1999 *J. Appl. Phys.* **85** 4141
[76] Collins R W and Ferlauto A S 2005 *Handbook of ellipsometry* ed Irene E G and Tomkins H G (Norwich, NY: William Andrew)
[77] Collins R W, An I, Lee J and Zapien J A 2005 *Handbook of ellipsometry* ed Irene E G and Tomkins H G (Norwich, NY: William Andrew)
[78] Bruggeman D A G 1935 *Ann. Phys. (Lepzig)* **24** 636
[79] Fried M, Lohner T, Polgar O, Petrik P, Vazsonyi E, Barsony I, Piel J P and Stehle J L 1996 *Thin Solid Films* **276** 223
[80] Lohner T, Fried M, Petrik P, Polgar O, Gyulai J and Lehnert W 2000 *Mat. Sci. and Engineering* **B69-70** 182
[81] Petrik P, Cayrel F, Fried M, Lohner T, Polgár O, Gyulai J and Alquier D 2005 *J. Appl. Phys.* **97** 123514
[82] Fodor B, Cayrel F, Agocs E, Alquier D, Fried M and Petrik P 2014 *Thin Solid Films* **in press** DOI: 10.1016/j.tsf.2014.02.014